Channel coding and time-diversity for optical wireless links

Fang Xu, Ali Khalighi*, Patrice Caussé, Salah Bourennane

École Centrale Marseille, Institut Fresnel, UMR CNRS 6133,
Domaine Universitaire de Saint-Jérôme, 13397 Marseille cedex 20, France
* *Corresponding author: Ali.Khalighi@fresnel.fr*

Abstract: Atmospheric turbulence can cause a significant performance degradation in free space optical communication systems. An efficient solution could be to exploit the temporal diversity to improve the performance of the transmission link. Depending on the tolerable delay latency, we can benefit from some degree of time diversity that we can exploit by employing channel coding and interleaving. In this paper, we investigate the efficiency of several channel coding techniques for different time diversity orders and turbulence conditions. We show that a simple convolutional code is a suitable choice in most cases as it makes a good compromise between decoding complexity and performance. We also study the receiver performance when the channel is estimated based on some training symbols.

OCIS codes: 060.2605 Free-space optical communication, 060.4510 Optical communications

References and links

1. V. W. S. Chan, "Free-space optical communications," J. Lightwave Technol. **24**, 4750–4762 (2006).
2. D. J. T. Heatley, D. R. Wisely, I. Neild, and P. Cochrane, "Optical wireless: The story so far," IEEE Commun. Mag. **72**, 72–82 (1998).
3. H. A. Willebrand and B. S. Ghuman, "Fiber optics without fiber," IEEE Spectrum **40**, 41–45 (2001).
4. S. Bloom, E. Korevaar, J. Schuster, and H. Willebrand, "Understanding the performance of free-space optics," J. Opt. Net. **2**, 178–200 (2003).
5. D. Kedar and S. Arnon, "Urban optical wireless communication networks: the main challenges and possible solutions," IEEE Commun. Mag. **42**, 2–7 (2004).
6. S. Arnon, "Effects of atmospheric turbulence and building sway on optical wireless communication systems," Opt. Lett. **28**, 129–131 (2003).
7. A. Harris, J. J. Sluss, H. H. Refai, and P. G. LoPresti, "Alignment and tracking of a free-space optical communications link to a UAV," Proc. Digital Avionics Syst. Conf. (DASC) **1.C**, 2.1–2.9 (2005).
8. V. I. Tatarskii, *Wave Propagation in a Turbulent Medium* (Dover Publications Inc., 1968). New York.
9. L. C. Andrews and R. L. Phillips, *Laser Beam Propagation through Random Media* (SPIE Press, Bellingham, Washington, 2005), 2nd ed.
10. J. G. Proakis, *Digital Communications* (McGraw-Hill, 5th edition, 2008).
11. F. S. Vetelino, C. Young, L. C. Andrews, and J. Recolons, "Aperture averaging effects on the probability density of irradiance fluctuations in moderate-to-strong turbulence," Appl. Opt. **46**, 2099–2108 (2007).
12. L. C. Andrews, R. L. Phillips, and C. Y. Hopen, "Aperture averaging of optical scintillations: power fluctuations and the temporal spectrum," Waves Random Media **10**, 5370 (2000).
13. E. J. Lee and V. W. S. Chan, "Part 1: Optical communication over the clear turbulent atmospheric channel using diversity," IEEE J. Sel. Areas Commun. **22**, 1896–1906 (2004).
14. S. G. Wilson, M. Brandt-Pearce, Q. L. Cao, and M. Baedke, "Optical repetition MIMO transmission with multipulse PPM," IEEE J. Sel. Areas Commun. **23**, 1901– 1910 (2005).
15. S. G. Wilson, M. Brandt-Pearce, Q. Cao, and J. H. Leveque, "Free-space optical MIMO transmission with Q-ary PPM," IEEE Trans. Commun. **53**, 1402–1412 (2005).
16. J. A. Anguita, I. B. Djordjevic, M. A. Neifeld, and B. V. Vasic, "Shannon capacities and error-correction codes for optical atmospheric turbulent channels," J. Opt. Net. **4**, 586–601 (2005).

#103396 - $15.00 USD Received 29 Oct 2008; revised 19 Dec 2008; accepted 19 Dec 2008; published 12 Jan 2009

17. J. W. Goodman, *Statistical Optics* (John Wiley & Sons, 1985). New York.
18. L. C. Andrews and R. L. Phillips, "I-K distribution as a universal propagation model of laser beams in atmospheric turbulence," J. Opt. Soc. Am. **2**, 160–163 (1985).
19. L. C. Andrews, R. L. Phillips, C. Y. Hopen, and M. A. Al-Habash, "Theory of optical scintillation," J. Opt. Soc. Am. **16**, 1417–1429 (1999).
20. M. A. Al-Habash, L. C. Andrews, and R. L. Phillips, "Mathematical model for the irradiance probability density function of a laser beam propagating through turbulent media," Opt. Eng. **40**, 1554–1562 (2001).
21. R. M. Gagliardi and S. Karp, *Optical Communications* (John Wiley & Sons, 1995), 2nd ed.
22. X. Zhu and J. Kahn, "Free-space optical communication through atomospheric turbulence channels," IEEE Trans. Commun. **50**, 1293–1330 (2002).
23. M. Cole and K. Kiasaleh, "Signal intensity estimators for free-space optical communications through turbulent atmosphere," IEEE Photon. Technol. Lett. **16**, 2395–2397 (2004).
24. X. Zhu and J. M. Kahn, "Pilot-symbol assisted modulation for correlated turbulent free-space optical channels," Proc. Soc. Photo-Opt. Instrum. Eng. **4489**, 138–145 (2002).
25. J. Hagenauer, E. Offer, and L. Papke, "Iterative decoding of binary block and convolutional codes," IEEE Trans. Inf. Theory **42**, 429–445 (1996).
26. *Digital Video Broadcasting (DVB); Framing Structure, Channel Coding and Modulation for Digital Terrestrial Television* (ETSI EN 300 744 V1.5.1, European Standard (Telecommunications series), 2004).
27. C. Berrou and A. Glavieux, "Near optimum error correcting coding and decoding: turbo-codes," IEEE Trans. Commun. **44**, 1261–1271 (1996).
28. F. Xu, M. A. Khalighi, P. Caussé, and S. Bourennane, "Performance of coded time-diversity free-space optical links," Proc. Queen's 24th Biennial Symp. Commun. (QSBC) pp. 146–149 (2008). Kingston, Canada.
29. F. Babich and F. Vatta, "On rate-compatible punctured turbo codes design," EURASIP J. Appl. Signal Process. **6**, 784–794 (2005).
30. A. S. Barbulescu and S. S. Pietrobon, "Interleaver design for turbo codes," Elect. Lett. **30**, 2107–2108 (1994).
31. N. Cvijetic, S. G. Wilson, and R. Zarubica, "Performance evaluation of a novel converged architecture for digital-video transmission over optical wireless channels," J. Lightwave Technol. **25**, 3366–3373 (2007).

1. Introduction

Free space optics (FSO) is a promising solution for the need to very high data rate point-to-point communication [1]. In an FSO system, the information-bearing laser beam is projected to the optical receiver along a line-of-sight. FSO has numerous advantages over radio-frequency (RF) technology [2, 3, 4] such as very high optical bandwidth, high transmission security, and interference immunity. FSO systems have attracted considerable attention since a few years for a variety of applications and markets, e.g. last mile connectivity, optical-fiber backup, entreprise connectivity, etc. [5].

Regarding the implementation of an FSO link, however, we are faced to several practical problems. First, the stringent line-of-sight requirement necessitates careful pointing and probably some tracking mechanisms at the receiver [6, 7]. Another important problem is the susceptibility of the optical link to weather conditions. In fact, aerosol scattering effects caused by rain, snow, and fog, can reduce the link range due to the propagation loss in non-clear atmosphere [8]. Even in clear sky conditions, inhomogeneities in the temperature and pressure of the atmosphere caused by solar heating and wind, lead to the variations of the air refractive index along the transmission path. The atmospheric turbulence, also called scintillation, causes random fluctuations in both the amplitude and the phase of the received signal, what we call *channel fading*. This leads to an increase in the link error probability. A comprehensive survey of optical-propagation effects can be found in [9].

In this paper, we assume that the transmitter and the receiver are perfectly aligned, and do not consider effects such as building sway. Also, we neglect the atmospheric losses associated with visibility, and focus on mitigating the channel fading arising from scintillation.

In general, channel coding (also called error correcting coding) is used to increase the robustness of a communication system against noise and interference [10]. However, it is well known that channel coding is not sufficient to mitigate channel fading efficiently. More efficient solutions are diversity techniques, e.g. in space, time, or frequency (wavelength). In its simplest

#103396 - $15.00 USD Received 29 Oct 2008; revised 19 Dec 2008; accepted 19 Dec 2008; published 12 Jan 2009

form, spatial diversity consists in aperture averaging when the receiver lens aperture is larger than the fading correlation length [9, 11]. Even with a relatively small lens, we can benefit from some aperture averaging in practice, especially in the case of strong turbulence [11, 12]. Better scintillation reduction is obtained by using multiple lenses at the receiver and/or multiple beams at the transmitter [13, 14]. Also, wavelength division multiplexing allows to benefit from frequency diversity. Here, we consider the case where, due to complexity or cost reduction, we work with a monochromatic laser, a single beam at the transmitter, and a single lens at the receiver. Also, we assume that we cannot benefit from any aperture averaging and the only possible diversity source is time diversity. The assumption of the absence of other sources of diversity permits to study the effect of time diversity alone. So, considering burst-mode data transmission, when the data frame length is large, compared to the channel coherence interval, we can exploit this time diversity by employing channel coding and interleaving. The data frame length equals, in fact, the interleaver depth used at the transmitter. Note that, by channel coherence interval, we mean the channel coherence time normalized by the symbol duration. The degree of time diversity equals the ratio of the frame length chosen for data transmission to the channel coherence interval. Note that, we can *potentially* benefit from such degree of time diversity but, in general, we may not attain full diversity just by performing channel coding and interleaving. Meanwhile, we also benefit from some channel coding gain. That is why we use the term *potential* time diversity order (PTDO).

Our aim in this work is to evaluate the performance improvement by time diversity in weak, moderate, and strong turbulence regimes. For this purpose, we consider four well-known channel coding methods, usually employed in optical communication systems: convolutional codes, Reed-Solomon (RS) codes, concatenated convolutional and RS (CCRS) codes, and turbo-codes (TC). We consider a realistic statistical channel model that is recently proposed for optical wireless systems, i.e., the gamma-gamma ($\Gamma\Gamma$) model [9]. Also, we consider the *frozen* channel model over the duration of several consecutive symbols [15]. This is also known as the *block-fading* model. We will compare the system performance in terms of the average bit error rate (BER) for the different coding solutions and take a close look at the efficiency brought by time diversity with channel coding and interleaving.

Note that a similar study is presented in [16], where the channel is modelled as uncorrelated ergodic. In other words, the channel coherence time can be considered to correspond to a single symbol duration. One may also consider the results in [16] as corresponding to the case of an infinite interleaver depth. In practice, however, channel time variations are not so fast and the interleaver depth can not be infinite either. As a result, we can benefit from far less time diversity; that is what we consider in this work, in contrast to the work in [16]. The results in [16] can, in fact, be considered as lower bounds on the system performance.

We consider the on-off keying (OOK) modulation. For optimal signal detection that we consider, we need the channel knowledge at the receiver. So, at a first step, we consider perfect channel knowledge at the receiver, and at a second step, we consider the case where the channel fading coefficients are estimated at the receiver based on some training (pilot) symbols.

The remainder of the paper is organized as follows. In Section 2, we present our modelling assumptions concerning the transmitter, channel, and the receiver. In Section 3, we describe the *soft* symbol detection at the receiver. We also explain the need to channel knowledge, as well as the channel estimation based on some training symbols. A brief review of the different coding solutions that we consider in this work is presented in Section 4. Numerical results are provided in Section 5 to compare the system performance for different coding solutions and under different conditions of turbulence and time diversity. Finally, Section 6 concludes the paper.

#103396 - $15.00 USD Received 29 Oct 2008; revised 19 Dec 2008; accepted 19 Dec 2008; published 12 Jan 2009

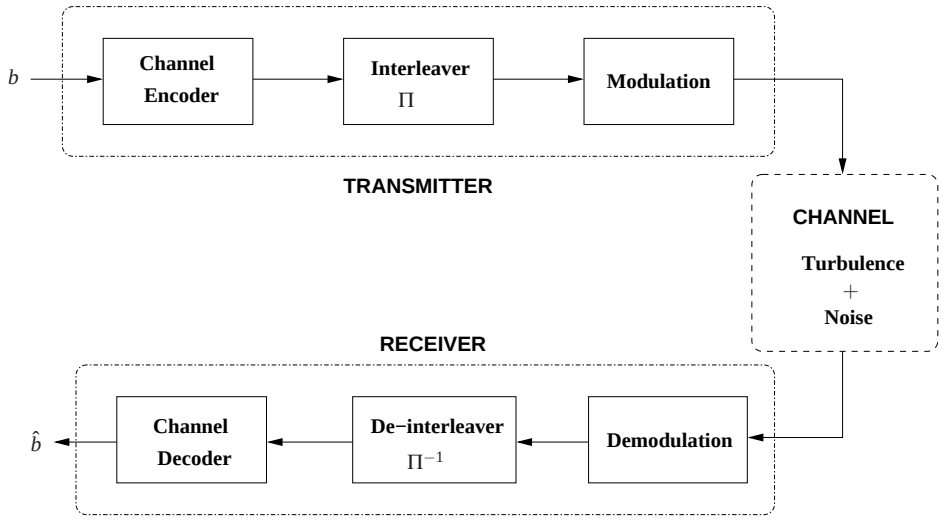

Fig. 1. System block diagram.

2. System model

The general system block diagram is given in Fig. 1. Each of the three main blocks of "Transmitter," "Channel," and "Receiver" are described in the following.

2.1. Transmitter

The equiprobable binary data bits b from the information source are passed through the channel encoder. The encoded bits are then interleaved before being converted to symbols (the modulation block) and transmitted through the channel. We consider pseudo-random interleaving in this work by which the encoded bits are permuted in a random manner (but known at the receiver). Better results can be obtained by optimizing the interleaver with respect to the channel time variations, however. By performing channel coding and interleaving, we can benefit from some degree of channel time diversity, which depends on the channel coherence interval and the frame length chosen for data transmission.

For the sake of implementation simplicity, we consider intensity modulation with direct detection (IM/DD), as it is used in most current optical communication systems. Also, we consider the most commonly used intensity modulation technique, that is, the non-return to zero (NRZ) OOK. So, the presence of an impulse of duration T_s represents a binary bit 1 (On state), whereas the absence of signal for the same duration represents a binary bit 0 (Off state).

2.2. Channel

The main impediment introduced by the channel that we consider here, is the scintillation. We consider the time variations according to the theoretical block-fading model, where the channel fade remains constant during a block (corresponding to the channel coherence interval) and changes to a new independent value from one block to next. In other words, channel fades are assumed to be independent and identically distributed (IID).

Several statistical models have been proposed so far for scintillation [17, 18, 19, 20]. Owing to its simplicity, the log-normal distribution is the most widely used, although its applicability is mainly restricted to weak turbulence conditions [17, 20]. On the contrary, the negative expo-

#103396 - $15.00 USD Received 29 Oct 2008; revised 19 Dec 2008; accepted 19 Dec 2008; published 12 Jan 2009

nential model fits well the strong turbulence conditions [20]. Here, we use the ΓΓ model that suitably describes both strong and weak turbulence regimes. By this model, the intensity fluctuation h induced by scintillation is modeled as a process in which small-scale (diffractive) intensity fluctuations are multiplicatively modulated by large-scale (refractive) fluctuations [19]. Let us denote by h_x and h_y the large- and small-scale irradiance fluctuations, respectively. h_x and h_y are assumed to be statistically independent and described by a gamma distribution. Based on these assumptions, the intensity fluctuation $h = h_x h_y$ has a ΓΓ distribution with the probability density function (PDF) as follows [9].

$$p(h) = \frac{2(\alpha\beta)^{(\alpha+\beta)/2}}{\Gamma(\alpha)\Gamma(\beta)} h^{(\alpha+\beta)/2-1} K_{\alpha-\beta}\left[2(\alpha\beta h)^{1/2}\right] \quad , \quad h > 0 \tag{1}$$

Here, α and β are the effective numbers of large- and small-scale eddies of the scattering environment, respectively, and $K_\alpha(x)$ is the modified Bessel function of the second kind and order α. Assuming plane wave propagation that is valid for relatively long-range applications, as well as turbulent eddies of zero inner scale, these parameters can be directly related to the atmospheric conditions [9, 20]:

$$\alpha = \frac{1}{\sigma_x^2} = \left[\exp\left(\frac{0.49\chi^2}{\left(1+1.11\chi^{12/5}\right)^{7/6}}\right) - 1\right]^{-1} \tag{2}$$

$$\beta = \frac{1}{\sigma_y^2} = \left[\exp\left(\frac{0.51\chi^2}{\left(1+0.69\chi^{12/5}\right)^{5/6}}\right) - 1\right]^{-1} \tag{3}$$

where σ_x^2 and σ_y^2 denote the variances of h_x and h_y, respectively, and $\chi^2 = 1.23 C_n^2 k^{7/6} L^{11/6}$ is the Rytov variance. Here, $k = 2\pi/\lambda$ is the wave number with λ the wavelength, and L is the link distance. Also, C_n^2 stands for the index of refraction structure parameter.

2.3. Receiver

At the receiver, after signal detection (the demodulator block) and de-interleaving, channel decoding is performed (see Fig. 1). The demodulation is performed based on the received signal light intensity. The electrical signal after the optical/electrical conversion is:

$$r_e = \eta\,(I + I_a) + n \tag{4}$$

where I is the received signal light intensity, I_a is the remaining ambient light intensity after frequency and spatial filtering [21], and η is the optical/electrical conversion efficiency. Also, n is the sum of thermal, dark, and shot noise. We assume that the ambient light can be almost perfectly cancelled [22]. So, after the cancellation of the ambient light, the received signal before demodulation is:

$$r = \eta I + n. \tag{5}$$

We suppose that the receiver is thermal noise limited, and consider n as a zero-mean Gaussian additive noise of variance σ_n^2, independent of the signal I. Let T_s denote the symbol duration and N_0 the noise unilateral power spectral density. Taking into account the low-pass filtering of bandwidth $1/2T_s$ after photo-detection, the noise variance equals $\sigma_n^2 = N_0/2T_s$. We further consider the received signal intensity I as the product of I_0, the emitted light intensity, and h, the channel atmospheric turbulence with the PDF given in (1):

$$I = h I_0. \tag{6}$$

#103396 - $15.00 USD Received 29 Oct 2008; revised 19 Dec 2008; accepted 19 Dec 2008; published 12 Jan 2009

The demodulator provides at its output logarithmic likelihood ratios (LLR) on the transmitted bits instead of hard values 0 or 1 (see Section 3 for more details). In other words, we perform *soft* signal detection. As we will explain in Section 4, in most cases, we perform *soft-input soft-output* (SISO) channel decoding, because as it is well known, soft decoding provides a better performance, compared to hard-decoding [10]. In such a case, the LLRs at the output of the demodulator are fed to the channel decoder, which in turn, provides LLRs on the information data bits at its output.

3. Soft detection of OOK symbols

The demodulation is done on the received signal r. Without loss of generality, let us assume $\eta = 1$. Also, let us replace I_0 by s that we consider as the transmitted symbol; it takes the values s_0 or s_1, corresponding to a transmitted bit 0 or 1, respectively. In our case of OOK modulation, $s_0 = 0$ (Off) and $s_1 = 1$ (On). At the receiver, we can make two hypotheses on the corresponding transmitted symbol:

$$\begin{cases} H_0 & : \quad r = hs_0 + n \\ H_1 & : \quad r = hs_1 + n \end{cases} \tag{7}$$

The decision we make in favor of H_0 or H_1 is based on the maximum *a posteriori* (MAP) criterion. Having assumed a Gaussian distribution for n, the conditional PDF of the received signal is:

$$P(r|s) = \frac{1}{\sqrt{2\pi\sigma_n^2}} \exp\left(\frac{-(r-hs)^2}{2\,\sigma_n^2}\right). \tag{8}$$

The MAP symbol detector provides the detected symbol $\hat{s}$ [10]:

$$\hat{s} = \arg\max_s P(r|s)\,P(s) \tag{9}$$

where $P(s)$ is the probability mass function of s. As we assumed equiprobable bits, (9) reduces to:

$$\hat{s} = \arg\max_s P(r|s). \tag{10}$$

To obtain $\hat{s}$, we calculate the likelihood ratio (LR) as follows.

$$\mathrm{LR} = \frac{P(r|s_1)}{P(r|s_0)} = \exp\left(\frac{-(r-hs_1)^2 + (r-hs_0)^2}{2\,\sigma_n^2}\right) = \exp\left(\frac{2hr - h^2}{2\,\sigma_n^2}\right). \tag{11}$$

If $\mathrm{LR} > 1$, we make the decision $\hat{s} = s_1$, and $\hat{s} = s_0$ otherwise. We can also use the LLR for decision making:

$$\mathrm{LLR} = \frac{2hr - h^2}{2\,\sigma_n^2} \underset{H_0}{\overset{H_1}{\gtrless}} 0 \tag{12}$$

In the case of hard signal detection, we provide $\hat{s}$ at the detector output.

3.1. Channel knowledge at the receiver

As we notice from (12), we need to know the instantaneous channel fading h for either soft or hard signal detection. In our performance analysis that we present in Section 5, we firstly suppose that the receiver is provided with the perfect channel state information (CSI). The perfect CSI, however, is rarely available at the receiver. In practice, some training (pilot) symbols are usually sent from the transmitter, based on which the receiver estimates the channel fading. By this approach, known as pilot symbol assisted modulation (PSAM), we reserve some positions in each frame for the transmission of pilots. As we consider the block-fading channel model in

#103396 - $15.00 USD Received 29 Oct 2008; revised 19 Dec 2008; accepted 19 Dec 2008; published 12 Jan 2009

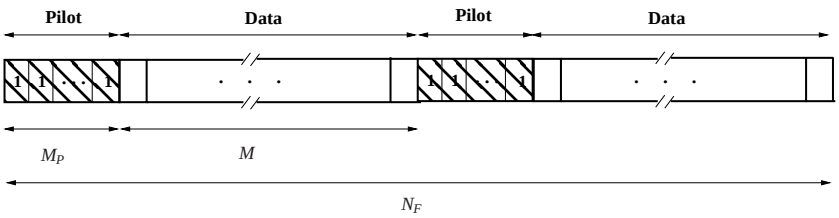

Fig. 2. Pilot insertion for channel estimation purpose; example of two fading blocks per frame of N_F symbols, $N_F = 2(M + M_P)$.

this work, we allocate M_P On-state OOK pilot symbols per fading block [23]. As an example, we have shown the pilot insertion in Fig. 2 for the case of two channel fades per frames of N_F symbols. The loss in the transmission rate due to pilot insertion is then $M_P/(M + M_P)$, where M denotes the number of data symbols corresponding to a fading block. In practice, pilots are rather distributed among data symbols [24]. However, as we consider the frozen channel model, the position of pilots in a block has no importance here. If we denote by r_i, $i = 1, \cdots, M_P$, the received symbol corresponding to the ith pilot symbol in a given fading block, the corresponding maximum likelihood channel estimate $\hat{h}$ is:

$$\hat{h} = \frac{1}{M_P} \sum_{i=1}^{M_P} r_i \ . \tag{13}$$

4. Review of channel coding and decoding techniques

In this section, we present the four channel coding techniques that we consider in this work, i.e., convolutional, RS, CCRS, and TC. As they are rather classical and well-known, we only present a brief review of them.

4.1. Convolutional codes

Convolutional codes are powerful error correcting codes usually used in digital communication systems. We consider recursive systematic convolutional (RSC) codes of constraint length K and denote the coding rate by R_c. At the receiver, we perform *soft* decoding based on SOVA (soft-output Viterbi algorithm) [25], which takes at its input the LLRs on the transmitted bits (coming from the demodulator) and provides at its output LLRs on the transmitted information bits.

4.2. Reed-Solomon codes

RS codes belong to the family of linear block codes and are usually used in data transmission systems submitted to burst errors such as satellite communications. We consider an RS encoder taking k data *symbols* of t bits each at input, and provides $n = 2^t - 1$ output *symbols*, by adding $n - k$ parity *symbols* to them. We denote it by RS(n,k). We consider here hard RS decoding which is used in most systems.

4.3. Concatenated convolutional and RS codes (CCRS)

Convolutional codes are efficient specially when errors caused by the communication channels are statistically independent. For the FSO channel, however, we are subject to burst errors due to fading. A more efficient coding scheme can be obtained by concatenating convolutional and RS codes as shown in Fig. 3. This is, for instance, what is defined in the DVB-S (Digital Video

#103396 - $15.00 USD Received 29 Oct 2008; revised 19 Dec 2008; accepted 19 Dec 2008; published 12 Jan 2009

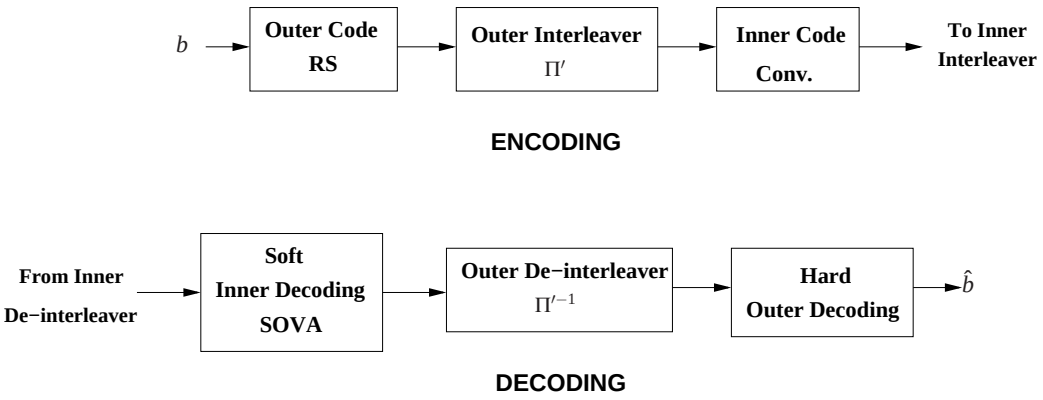

Fig. 3. Concatenation of RS and convolutional codes. ENCODING and DECODING correspond to the "Channel Encoder" and "Channel Decoder" blocks in Fig. 1, respectively.

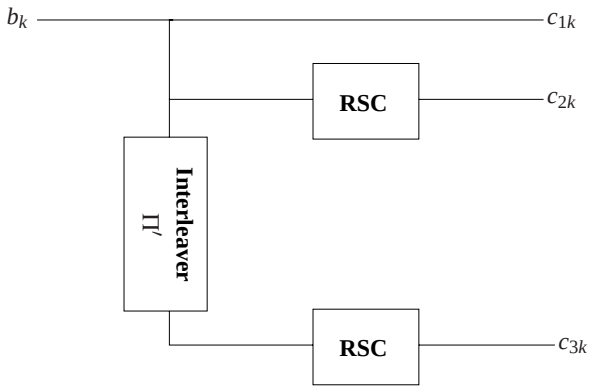

Fig. 4. Turbo encoder block diagram.

Broadcasting - Satellite) standard [26]. Encoded data by the outer (RS) code are first interleaved by an *outer* interleaver Π' before passing to the inner (convolutional) encoder. The resulting bits are then permuted by the *inner* (channel) interleaver (the block Π in Fig. 1) before being mapped to symbols. The inner interleaving and modulation are done according to the block diagram of Fig. 1. At the receiver, after soft symbol detection and channel (inner) de-interleaving (see Fig. 1), we first perform SISO decoding of the inner (convolutional) code based on SOVA, as shown in Fig. 3. Next, after outer de-interleaving, we perform hard decoding of the outer (RS) code.

4.4. Turbo-codes

Turbo-codes are powerful codes that can provide performances close to the Shannon limit [27]. We consider the parallel concatenation of two identical RSC codes, as shown in Fig. 4. For each information bit b_k, at the encoder output we get the systematic bit c_{1k} as well as two parity bits c_{2k} and c_{3k}, provided by the two RSC encoders. The overall coding rate R_c is then 1/3. Notice that this corresponds to the "Channel Encoder" block in Fig. 1.

In contrast to our previous work [28], here, in order to perform a fair comparison between different channel codes, we set the channel coding rate R_c to 1/2 for all coding schemes, as we

#103396 - $15.00 USD Received 29 Oct 2008; revised 19 Dec 2008; accepted 19 Dec 2008; published 12 Jan 2009

will explain in the next section. For this purpose, we puncture the turbo encoder output bits. Puncturing is done on the parity bits, i.e., the output bits c_{2k} and c_{3k} in Fig. 4, and all systematic bits are kept. A special attention should be devoted to the design of the outer interleaver Π'. We perform a homogeneous puncturing [29], through the use of a so-called *odd-even* interleaver [30] that ensures that each information bit has exactly one of its parity bits. In other words, punctured bits are evenly spread among c_{2k} and c_{3k} parity bits. As a result, the error correction capability of the code is uniformly distributed over all information bits.

Turbo decoding, on the other hand, consists in decoding the two RSC codes in an iterative (*turbo*) manner, by using two SISO decoders exchanging *extrinsic* LLRs between them (see [27] for more details). Again we consider SOVA-based SISO decoding. At the first iteration, we set the LLRs corresponding to punctured bits to zero.

5. Numerical results

In this section, we present some simulation results to compare the performances of the proposed coding schemes under different conditions of turbulence. The system performance is evaluated in terms of BER as a function of signal-to-noise ratio (SNR). We consider the electrical SNR in the form of E_b/N_0, where E_b is the averaged received energy per *information* bit. We consider communication by burst, where frames of N_F OOK modulated symbols are transmitted through the channel. Also, the inner (channel) interleaver is pseudo-random and of depth N_F. Note that for the case of RSC or turbo coding, N_F includes the trellis termination bits. In the following, we provide details on the other simulation parameters. Note that, as we use OOK modulation, we may interchangeably use the words 'bit' and 'symbol.'

5.1. Coding schemes

To do a fair comparison of the performances of different coding schemes, we set the R_c to 1/2 for all coding schemes. We chose this rate for simplicity as it corresponds to the coding rate for the CCRS and RSC schemes that we consider here. As the convolutional code, we mainly consider the RSC code $(1, 15/17)$ of constraint length $K = 4$. Numbers 15 and 17 represent the code polynomial generators in octal. As the RS code, we use the code $\mathrm{RS}(255, 127)$ of rate $R_c = 127/255 \approx 0.5$, for which $t = 8$. For the case of CCRS coding, we use the RSC code (1,133/171) of $K = 7$ as the inner code and $\mathrm{RS}(255, 239)$ as the outer code. We have $R_c \approx 0.46$, close enough to 0.5. This scheme corresponds to that proposed in the DVB-S standard-2004 [26]. After RS coding, we perform pseudo-random outer interleaving of depth $N_F/2$ before convolutional coding (Π' in Fig. 3). Note that, in contrast to the scheme proposed in [26], we do not consider the *shortened* code $\mathrm{RS}(204, 188, t = 8)$ nor the special cyclic byte-wise outer interleaving. In fact, in DVB-S, the special outer interleaver tries to benefit from the channel time diversity, whereas the inner interleaver tries rather to benefit from the frequency diversity with the OFDM scheme used. Lastly, for the TC case, we consider the parallel concatenation of two identical RSC codes $(1, 15/17)$ with the puncturing pattern as explained in Subsection 4.4 to obtain $R_c = 0.5$. Only two iterations are processed for turbo-decoding. In fact, for the punctured TC and at the presence of channel turbulence, we obtain negligible performance improvement with more iterations.

For the sake of brevity, in what follows, we will refer to these four coding schemes as RSC4 (with reference to K), RS, CCRS, and TC, respectively. Also, the minimum frame size that we consider in our simulations is $N_F = 4080$, because it is the minimum N_F for the case of CCRS coding: At the RS encoder output we have $255 \times 8 = 2040$ coded bits, then, after RSC encoding of rate 1/2, we obtain 4080 coded bits (excluding trellis termination).

#103396 - $15.00 USD Received 29 Oct 2008; revised 19 Dec 2008; accepted 19 Dec 2008; published 12 Jan 2009

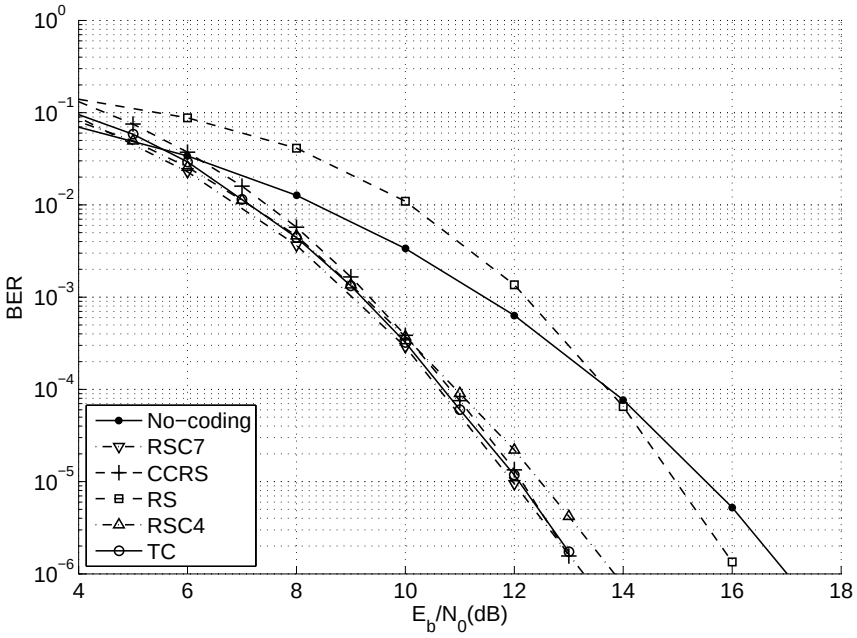

Fig. 5. Weak turbulence conditions, $(\alpha = 51.9\,, \beta = 49.1)$, no time diversity, perfect CSI.

5.2. Turbulence modelling

As we explained in Section 2, we consider the block-fading model for channel time variations. Also, fade statistics are considered according to the $\Gamma\Gamma$ model with the parameters α and β, given by (2) and (3), respectively.

We consider three typical cases of weak, moderate, and relatively strong turbulence conditions for which we set χ to 0.2, 1, and 3, respectively, as suggested in [16]. Although in general, there may be no direct relationship between the turbulence strength and the channel time correlation, we consider three channel coherence times of 1ms, 100μs, and 20μs, for the cases of weak, moderate, and strong turbulence regimes, respectively. We will later explain that the results that we present remain general, as they mainly depend on the potential time diversity order.

5.3. Case of perfect channel knowledge at the receiver

5.3.1. Weak turbulence conditions

Let us first consider the case of $\chi = 0.2$ that results in $\alpha = 51.9$ and $\beta = 49.1$. We set the data rate to $R = 1$ Gbps that corresponds to the symbol duration $T_s = 1$ns. Also, we consider the typical channel coherence time of $\tau_c = 1$ms for this case that means that the channel varies over blocks of $N_c = \tau_c/T_s = 10^6$ symbols, according to our block-fading channel model. First consider the frames of length $N_F = 4080$ for which we cannot benefit from any time diversity. To see the efficiency of different codes (in the sense of coding gain), we have presented in Fig. 5 the curves of BER versus E_b/N_0 for different coding schemes, as well as for the case where no channel coding is performed. We can see that the RS code is not really efficient. This poor performance is principally due to hard decoding [31]. However, the three other codes provide interesting and almost identical performance improvements. For instance, at BER=

#103396 - $15.00 USD Received 29 Oct 2008; revised 19 Dec 2008; accepted 19 Dec 2008; published 12 Jan 2009

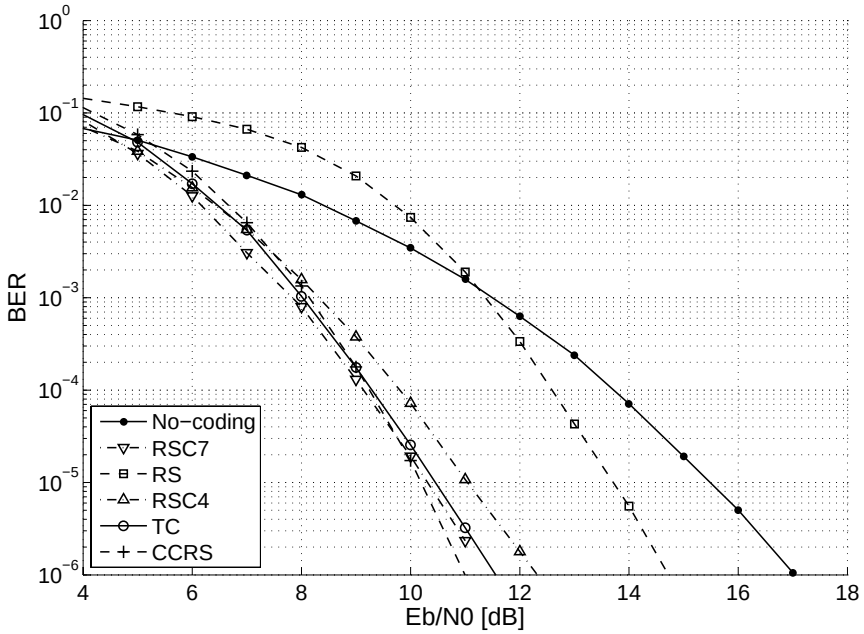

Fig. 6. Weak turbulence conditions, $(\alpha = 51.9\,,\, \beta = 49.1)$, PTDO = 2, perfect CSI.

10^{-5}, compared to the no-coding case, we obtain a gain of 0.6 dB and 3 dB in SNR by using the RS and RSC4, respectively, and a gain of 3.4 dB for CCRS, and TC. For the sake of comparison, we have also shown the BER curve for the $(1, 133/171)$ RSC code that we note by RSC7. We note that its performance is almost the same as that of CCRS scheme.

In the present case, in order to obtain a *potential* time diversity order (PTDO) of 2, we have to set the frame length N_F to about 2×10^6 symbols, which corresponds to a delay-latency of 2ms. The corresponding performance curves are shown in Fig. 6. Since without coding, we cannot benefit from this diversity, we obtain the same performance for the no-coding case as in Fig. 5. We notice a considerable performance gain by performing channel coding. For instance, at BER$= 10^{-5}$, compared to the no-coding case, we have an SNR gain of 1.8 dB, 4.4 dB, 5 dB, 5.2 dB and 5.4 dB, by using RS, RSC4, TC, RSC7 and CCRS, respectively. Notice that we cannot explain the slopes of the BER curves as we cannot distinctly dissociate diversity and coding gains. The best performance is obtained for CCRS, that is principally due to the use of RSC7 code in its structure, the performances of RSC7 and CCRS being almost identical. However, the decoding complexity of RSC7 is much higher that RSC4, as it grows exponentially with K. The decoding complexity of TC, on the other hand, is almost 4 times that of RSC4, as we perform only two decoding iterations.

Given the results of Figs. 5 and 6, we see that a good compromise between performance and complexity is achieved by using RSC4. So, we recommend the RSC4 scheme as the suitable solution for relatively weak turbulence conditions.

5.3.2. Moderate turbulence conditions

For this case, we consider $\chi = 1$ that results in $\alpha = 4.39$ and $\beta = 2.56$. We set the data rate to $R = 200$ Mbps that corresponds to $T_s = 5$ns. The reason of considering a lower data rate

#103396 - $15.00 USD Received 29 Oct 2008; revised 19 Dec 2008; accepted 19 Dec 2008; published 12 Jan 2009

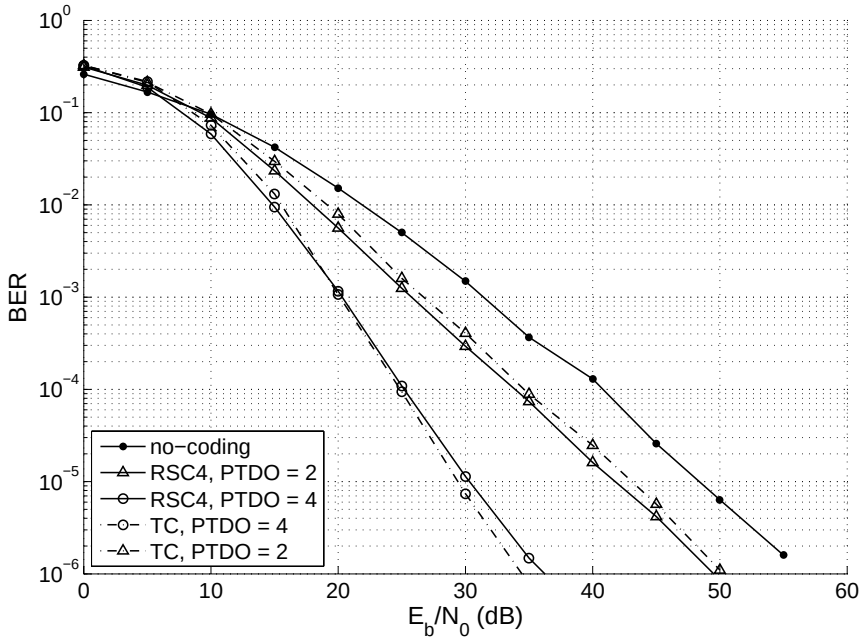

Fig. 7. Moderate turbulence conditions, $(\alpha = 4.39, \beta = 2.56)$, PTDO = 2 and 4, perfect CSI.

compared to the previous case is that, in practice, lower transmission rates are used in the case of stronger turbulence. We consider the typical channel coherence time of $\tau_c = 100\mu$s for this case. So, the channel will change over blocks of $N_c = \tau_c/T_s = 20000$ symbols. If we benefit from no time diversity, all coding schemes have poor performances, close to the no-coding case (results are not presented). That is quite logical, because for the frames undergoing a severe fading, channel coding alone is not efficient.

If, for instance, we want to benefit from a PTDO of 2 in this case, we have to set the frame length to about 40000 symbols. This will impose a delay-latency of 200μs. The corresponding performance curves are shown in Fig. 7. The curve representing the no-coding case can also be regarded as that with no diversity. We have only shown the BER curves for RSC4 and TC for which we notice a considerable performance improvement. For instance, at BER=10^{-5}, we have a gain of about 6.6 dB and 5.3 dB in SNR, by using RSC4 and TC, respectively. The simple RS code is not efficient at all under moderate turbulence conditions. In fact, frames experiencing a locally severe fading have an important impact on the average BER. For those frames, the RS code does not provide any improvement. Also, the performances of CCRS and RSC7 are almost equivalent to that of RSC4.

To benefit from a PTDO of 4, we have to set the frame length to about 80000 symbols and undergo a delay-latency of 400μs. The corresponding curves in Fig. 7 show that, at BER=10^{-5}, we obtain substantial gains of about 18.1 dB and 19 dB in SNR, by using RSC4 and TC, respectively. Notice that, TC now outperforms RSC4, in contrast to the case of PTDO=2. This can be explained by the fact that puncturing the turbo-code is particularly penalizing for those blocks undergoing a relatively severe fade. With a larger PTDO, fading is *averaged* more and such severe local fades occur much less frequently. So, TC finds its error correcting superiority over the simple convolutional code.

#103396 - $15.00 USD Received 29 Oct 2008; revised 19 Dec 2008; accepted 19 Dec 2008; published 12 Jan 2009

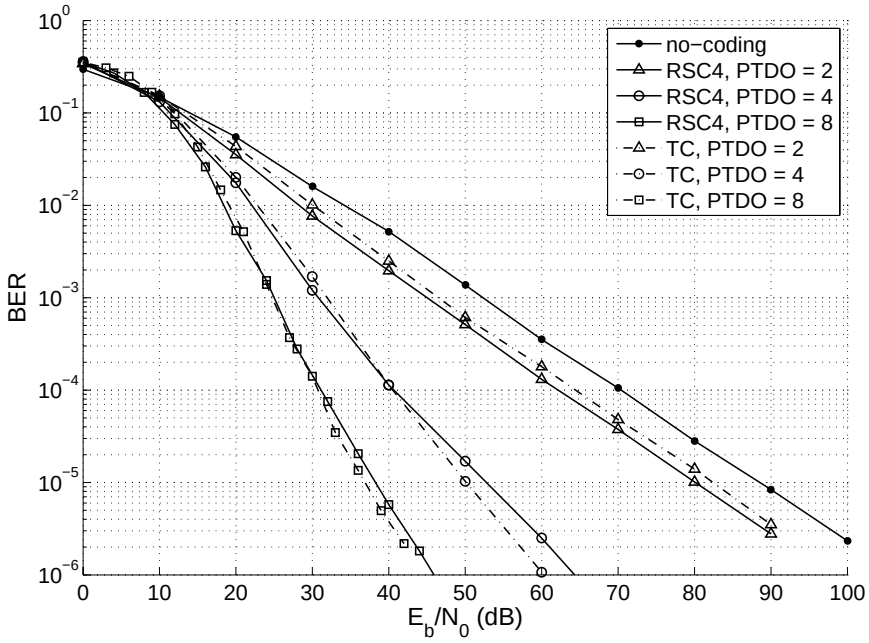

Fig. 8. Strong turbulence conditions, $(\alpha = 5.49, \beta = 1.12)$, PTDO = 2, 4, and 8, perfect CSI.

5.3.3. Strong turbulence conditions

For this case, we set $\chi = 3$ that results in $\alpha = 5.49$ and $\beta = 1.12$ in the $\Gamma\Gamma$ channel model. We consider the data rate of $R = 100$ Mbps that corresponds to the symbol duration $T_s = 10$ns, and the channel coherence time of $\tau_c = 20\mu$s. According to our block-fading channel model, the channel changes over blocks of $N_c = \tau_c/T_s = 2000$ symbols. We consider three cases of symbol-frame-lengths of about 4000, 8000, and 16000 symbols, where, respectively, we have a PTDO of about 2, 4, and 8, and a delay-latency of about 40μs, 80μs, and 160μs. Results are shown in Fig. 8, where only the cases of no-coding, RSC4, and TC are shown. Again, the BER curve for the case of no-coding is practically equivalent to the case of coding with no diversity. We exclude the case of simple RS encoding, as we noticed previously that it is not efficient. Also, the CCRS scheme has practically no interest as its performance is very close to that of RSC4. We notice that RSC4 is particularly efficient; the performance improvements at BER=10^{-5} with respect to the no-coding case are about 8.4 dB, 35.8 dB, and 50.2 dB, for PTDO of 2, 4, and 8, respectively. A similar behavior is observed for TC with respect to RSC4: it outperforms RSC4 for PTDO of 4 and 8.

Given the results of Figs. 7 and 8, we recommend the use of a simple convolutional code for moderate to strong turbulence conditions: Although for higher PTDO we achieve a larger gain by using the TC scheme, globally, the convolutional code appears to be more adequate as it makes a good compromise between performance and decoding complexity.

5.3.4. Discussion on the diversity gain

The improvement in the receiver performance does not depend only on PTDO, but also on the coding rate R_c and the interleaver design.

#103396 - $15.00 USD Received 29 Oct 2008; revised 19 Dec 2008; accepted 19 Dec 2008; published 12 Jan 2009

It is important to note that the presented results are valid for pseudo-random interleaving. For this reason, when PTDO=2, we do not attain an effective diversity of 2 and the slopes of the corresponding BER curves are not twice as those of no-diversity. We could instead consider perfect interleaving to benefit from almost full potential diversity: For PTDO=2, i.e., two channel fades h_1 and h_2 per frame, and convolutional coding, perfect interleaving can be done by simply sending the systematic bits on h_1 and the redundant bits on h_2, for example. However, the reason we considered pseudo-random interleaving with the block-fading channel model is that the results represent better the real case: In practice, channel varies continuously in time and interleaving cannot be perfect. On such a channel, any interleaving can benefit only partly from time diversity. For faster channel time variations (equivalent to a larger PTDO in our theoretical model), we can benefit more from time diversity. This is in accordance with what we observed from Figs. 7 and 8.

The channel coding rate R_c is also an important parameter. As we set R_c to 1/2 for all coding schemes, by increasing PTDO, we do not benefit from full diversity and we can only approach an effective diversity order of $1/R_c = 2$. For PTDO>2, more considerable performance improvements are obtained for lower R_c. This can be verified by referring to our previous work (Reference [28]), where we have considered a rate 1/3 turbo-code. Assuming perfect interleaving, to benefit from almost full potential diversity, we should set R_c to 1/PTDO. Note that, by reducing R_c, we reduce the information transmission rate as well. Then, there will be a compromise between the link margin and the information transmission rate.

5.4. Case of pilot-based channel estimation

Up to now, we have assumed that we have perfect CSI available at the receiver. It is interesting to study the receiver performance in a practical system where the channel is estimated based on some training pilots. Here, we are particularly interested to see the sensitivity of a given coding scheme to the channel estimation errors. For this purpose, for each coding scheme, we set the SNR to that results in BER=10^{-5} in the case of perfect channel knowledge. We then evaluate the BER for different number of pilot symbols. Remember from Subsection 3.1 that corresponding to each fading block of M data symbols, we transmit M_P pilot symbols.

Fig. 9 shows the BER curves versus M_P for the two cases of weak and strong turbulence conditions and the two coding schemes RSC4 and TC. For both cases, the PTDO is set to 2. We notice that, for the case of weak turbulence, TC is more sensitive to channel estimation errors than RSC4. Nevertheless, the interesting point is that, only few pilot symbols are sufficient to provide results close to the perfect channel knowledge case. In other words, we undergo a negligible loss in the data rate due to the transmission of training symbols.

For the case of strong turbulence, we notice that by setting $M_P = 2$, we are already quite close to the perfect-CSI case (results are shown only for TC). As a matter of fact, for the strong turbulence case, the average SNR to obtain a given BER is much higher than that for the weak turbulence regime (82.4 dB instead of 10.45 dB at BER=10^{-5}). So, for those frames experiencing a locally low fade, the channel is almost perfectly estimated. For locally severe fades, on the other hand, we are likely to lose the entire frame, irrespective of the quality of channel estimation.

It is interesting to compare the results of Fig. 9 to those already presented in a previous work (Reference [28], Fig. 3): we note that the RSC4 code is less sensitive to channel estimation errors than RSC7, which is quite reasonable. Also, the punctured (rate 1/2) turbo-code is less sensitive to estimation errors than the rate 1/3 turbo-code.

#103396 - $15.00 USD Received 29 Oct 2008; revised 19 Dec 2008; accepted 19 Dec 2008; published 12 Jan 2009

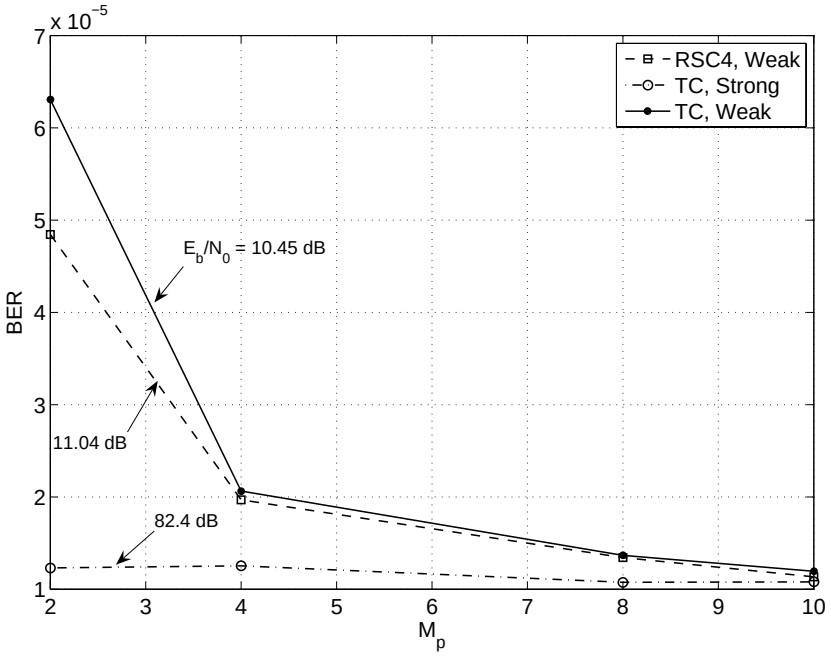

Fig. 9. BER versus the number of pilots per fading block. PTDO = 2, strong and weak turbulence conditions, BER=10^{-5} for perfect channel knowledge, $N_F = 4080$.

6. Conclusions and discussion

For an FSO transmission link submitted to different turbulence conditions, we performed a comparative study of the performances of different channel coding techniques, employed under the presence or not of time diversity. We showed that RS coding alone is not robust against (even weak) channel turbulence. For relatively weak turbulence, convolutional and turbo codes have almost identical performances and provide interesting performance improvements. Under moderate to strong turbulence conditions, these codes are quite efficient provided that we can benefit from some degree of time diversity. The CCRS scheme seems to have little interest in practice due to more decoding complexity and to the fact that its performance is very close to that of a convolutional code alone. Overall, we recommend a convolutional code as the suitable choice regarding the decoding complexity and the obtained performance. Lastly, we showed that a sufficient channel estimation precision is obtained by dedicating a very small percentage of the data rate to the transmission of pilot symbols.

To exploit the potential time diversity, channel coding should be done together with symbol interleaving. The interleaver depth should be as large as possible to bring a good diversity order. This, however, implies some delay latency and, more importantly, may require a large memory at the receiver that can not be adequate for a practical implementation of the system. In our study, we considered smaller channel coherence times for stronger turbulence conditions. However, the general results remain exploitable and the only factor to modify is the implied latency in signal transmission. In fact, since we considered the average BER as the performance evaluation criterion, results have little dependence on the actual frame length N_F, and the important factor is the potential diversity order. We have verified that, for the same potential diversity order, that is, the same ratio of N_F to the channel coherence interval, the presented performance

#103396 - $15.00 USD Received 29 Oct 2008; revised 19 Dec 2008; accepted 19 Dec 2008; published 12 Jan 2009

curves have little dependence on the actual N_F.

Finally, notice that in our previous work [28], we had considered a rate 1/3 turbo-code and compared its performance notably with rate 1/2 convolutional codes. The turbo-code had then much better performances than those presented in the present paper. The reason is that, a lower rate code can average more efficiently over the channel fades. To perform a fair comparison between different channel codes it is essential to use the same coding rate for all coding schemes, as we did in this paper.

Acknowledgment

The authors wish to thank Frédéric Chazalet from Shaktiware Co., Marseille, France, Noah Schwartz from ONERA, Chatillon, France, Jaime A. Anguita from University of Arizona, Tucson, AZ, and Steve Hranilovic from McMaster University, Hamilton, Canada, for their fruitful discussions. Parts of this paper have been presented in Queen's Binomial Conference on Communications (QSBC), Kingston, Canada, June 2008.

#103396 - $15.00 USD Received 29 Oct 2008; revised 19 Dec 2008; accepted 19 Dec 2008; published 12 Jan 2009